PNAS RESEARCH ARTICLE | NEUROSCIENCE

Germline knockout of *Nr2e3* protects photoreceptors in three distinct mouse models of retinal degeneration

Alexander V. Kolesnikov[a,1], Daniel P. Murphy[b,1], Joseph C. Corbo[b,2], and Vladimir J. Kefalov[a,2]

Edited by Jeremy Nathans, Johns Hopkins University School of Medicine, Baltimore, MD; received September 16, 2023; accepted January 17, 2024

Retinitis pigmentosa (RP) is a common form of retinal dystrophy that can be caused by mutations in any one of dozens of rod photoreceptor genes. The genetic heterogeneity of RP represents a significant challenge for the development of effective therapies. Here, we present evidence for a potential gene-independent therapeutic strategy based on targeting *Nr2e3*, a transcription factor required for the normal differentiation of rod photoreceptors. *Nr2e3* knockout results in hybrid rod photoreceptors that express the full complement of rod genes, but also a subset of cone genes. We show that germline deletion of *Nr2e3* potently protects rods in three mechanistically diverse mouse models of retinal degeneration caused by bright-light exposure (light damage), structural deficiency (rhodopsin-deficient *Rho*$^{-/-}$ mice), or abnormal phototransduction (phosphodiesterase-deficient *rd10* mice). *Nr2e3* knockout confers strong neuroprotective effects on rods without adverse effects on their gene expression, structure, or function. Furthermore, in all three degeneration models, prolongation of rod survival by *Nr2e3* knockout leads to lasting preservation of cone morphology and function. These findings raise the possibility that upregulation of one or more cone genes in *Nr2e3*-deficient rods may be responsible for the neuroprotective effects we observe.

retina | photoreceptors | retinitis pigmentosa

Significance

Retinitis pigmentosa (RP) is a common form of retinal degenerative disease that can be caused by mutations in any one of dozens of rod photoreceptor genes. The genetic heterogeneity of RP represents a significant challenge for the development of effective therapies. Here, we present evidence for a potential gene-independent therapeutic strategy based on targeting *Nr2e3*, a gene encoding a transcription factor required for the normal differentiation of rod photoreceptors. *Nr2e3*-deficient mouse rods express the normal complement of rod photoreceptor genes but also a subset of cone genes. We show that *Nr2e3*-deficient rods are remarkably resistant to degeneration in three mechanistically diverse RP models, suggesting that the upregulation of cone genes in *Nr2e3*-deficient rods has a strong neuroprotective effect.

Retinal degeneration affects millions of people worldwide and can be caused by mutations in any one of more than 250 genes (1–3). Retinitis pigmentosa (RP) is the most common form of retinal degeneration and can result from mutations in dozens of individual genes, many of which are rod-enriched or rod-specific (4, 5). While rods constitute the great majority of photoreceptors in most mammalian retinas including mice and humans, their loss has only relatively mild effects on human visual function which manifest as night blindness. The most severe consequence of rod degeneration is secondary cone loss which occurs via mechanisms that are still actively investigated (6). The death of cones, which mediate daytime vision, is particularly disabling for patients and represents the primary source of morbidity in RP. Therefore, preventing secondary cone loss is a key goal of therapy for patients with RP.

The genetic heterogeneity of RP represents a significant challenge for the development of effective treatments for this disease. For this reason, there is a strong motivation to develop gene-independent strategies that could be used to treat a wide range of genetic forms of RP (7, 8). One promising approach for creating a gene-independent therapy for RP is based on genetic reprogramming of rod photoreceptors. We showed previously that reprogramming adult rods into a cone-like state by acutely knocking out the rod-specific transcription factor *Nrl* delayed rod death and preserved native cones in a *rhodopsin* (*Rho*) knockout mouse model of retinal degeneration (9). Subsequent work extended these findings, showing that acute *Nrl* knockout makes rods resistant to the effects of mutations in multiple rod-specific genes (9–11). However, as *Nrl* is a key early-acting transcription factor in the rod transcription network (12, 13), its knockout causes a significant shift in the gene expression profile of rods that ultimately results in changes in their structural and functional properties (9). Moreover, mutations in *Nrl* itself are a known cause of RP in both mice and humans (14–17). For these reasons, we sought to identify additional genes downstream of *Nrl* that might be targeted therapeutically but without causing widespread changes in rod gene expression.

For this purpose, we decided to target *Nr2e3*, a transcription factor downstream of *Nrl* (12, 18). *Nr2e3* mutant mice (*Nr2e3*$^{rd7/rd7}$; subsequently referred to as "*rd7*") have hybrid rod photoreceptors that express the full complement of rod genes as well as a subset of cone genes (19, 20). Crucially, for our purpose, the hybrid rod photoreceptors of *rd7* mice have nearly normal rod-like morphology and physiology, as was previously shown (19, 21, 22). Accordingly, a future gene therapy approach targeting *Nr2e3* would be expected to be much less disruptive than knocking out *Nrl* and might both preserve rod function and prevent secondary cone loss.

Author affiliations: [a]Department of Ophthalmology, Gavin Herbert Eye Institute, University of California, Irvine, CA 92697; and [b]Department of Pathology and Immunology, Washington University School of Medicine, St. Louis, MO 63110

Author contributions: A.V.K., D.P.M., J.C.C., and V.J.K. designed research; A.V.K. and D.P.M. performed research; A.V.K., D.P.M., and J.C.C. analyzed data; and A.V.K., D.P.M., J.C.C., and V.J.K. wrote the paper.

The authors declare no competing interest.

This article is a PNAS Direct Submission.

[1]A.V.K. and D.P.M. contributed equally to this work.

[2]To whom correspondence may be addressed. Email: jcorbo@wustl.edu or vkefalov@hs.uci.edu.

This article contains supporting information online at https://www.pnas.org/lookup/suppl/doi:10.1073/pnas.2316118121/-/DCSupplemental.

Published March 5, 2024.

In the present work, we evaluated the feasibility of this idea by characterizing the effects of germline knockout of *Nr2e3* in three mouse models of photoreceptor degeneration including light-induced photoreceptor damage (23) and two models of RP which vary in rate of disease progression and mechanism: *Pde6b*$^{rd10/rd10}$ (subsequently referred to as "*rd10*") and *Rho*$^{-/-}$ (24–27). We show that *Nr2e3* knockout slows the degeneration and functional decline of rod cells in all three models, thereby preventing secondary cone death and preserving cone-mediated daylight vision. These experiments establish the feasibility of suppressing the expression *Nr2e3* in photoreceptors as a therapeutic strategy for treating a broad range of retinal degenerative disorders.

Results

Photoreceptors of *rd7* Mice Are Resistant to the Damaging Effects of Bright Light. To determine whether mutations in *Nr2e3* can protect rods against light-induced degeneration, we performed a series of light-damage experiments on 3-mo-old wild-type (WT) and *rd7* littermates. All mice used in these experiments were homozygous for the Leu-450 isoform of RPE65, which makes them more susceptible to light-induced photoreceptor loss (28). We exposed awake animals to bright white light (15 kLux) for 8 h, returned the animals to a normal light/dark cycle for 1 wk, and then analyzed their retinas by histology. This light damage (LD) regimen caused extensive death of rods in WT mice (Fig. 1*A*). The most severe rod loss (~73%) was observed in the central retina, immediately dorsal to the optic nerve head, whereas a lesser degree of loss was observed in the ventral–central retina (~44%). Overall, the peripheral retina was less affected (Fig. 1*C*). In stark contrast, *rd7* rods showed no appreciable evidence of degeneration after identical light exposure (Fig. 1 *B* and *D*). Moreover, cone arrestin immunoreactivity was largely extinguished in WT retinas but well-preserved in *rd7* mutants (Fig. 1 *A* and *B*).

To extend these findings and correlate them with changes in rod physiological function, we exposed mice to bright white light of three different intensities and evaluated scotopic retinal responses by in vivo electroretinogram (ERG) recordings 1 wk later. We first exposed WT and *rd7* mice to a 7.5-kLux light for 5 h (i.e., relatively low LD). One week after light exposure, WT mice experienced a ~40% reduction of the maximal rod-driven ERG a-wave (Fig. 2*A*) and an accompanying ~25% decline in maximal rod ON bipolar cell-driven ERG b-wave (*SI Appendix*, Fig. S1), relative to unexposed control animals. Remarkably, the same irradiation did not cause any reduction in the scotopic ERG a-wave responses of *rd7* mice (Fig. 2*B*); there was also no decline in the scotopic ERG b-wave (*SI Appendix*, Fig. S1). We next exposed mice to a 15-kLux light for 8 h (i.e., intermediate LD). Compared to the 7.5-kLux exposure, this treatment caused more severe reduction of both ERG a-wave (~75%; Fig. 2*C*) and b-wave (~50%; *SI Appendix*, Fig. S1) responses in WT animals, consistent with the substantial retinal degeneration observed in this condition (Fig. 1*A*). However, this brighter light exposure still did not affect either of these ERG components in *rd7* mice (a-waves in Fig. 2*D*). The analysis of cone contribution into dark-adapted ERG response indicated that this light regimen also caused a ~twofold decline of M-cone function in WT mice (from 110 ± 3 μV in unexposed group, n = 12, to 48 ± 18 μV in light-exposed animals, n = 10, $^{*}P < 0.05$). In contrast, the cone function was fully preserved in *rd7* mice under the same conditions (100 ± 16 μV for unexposed, n = 14; 95 ± 2 μV for irradiated animals, n = 10, $P > 0.05$). Last, we exposed mice to a 40-kLux light for 8 h (i.e., high LD). In WT mice, we observed a dramatic decrease of both scotopic ERG a-waves (Fig. 2*E*) and

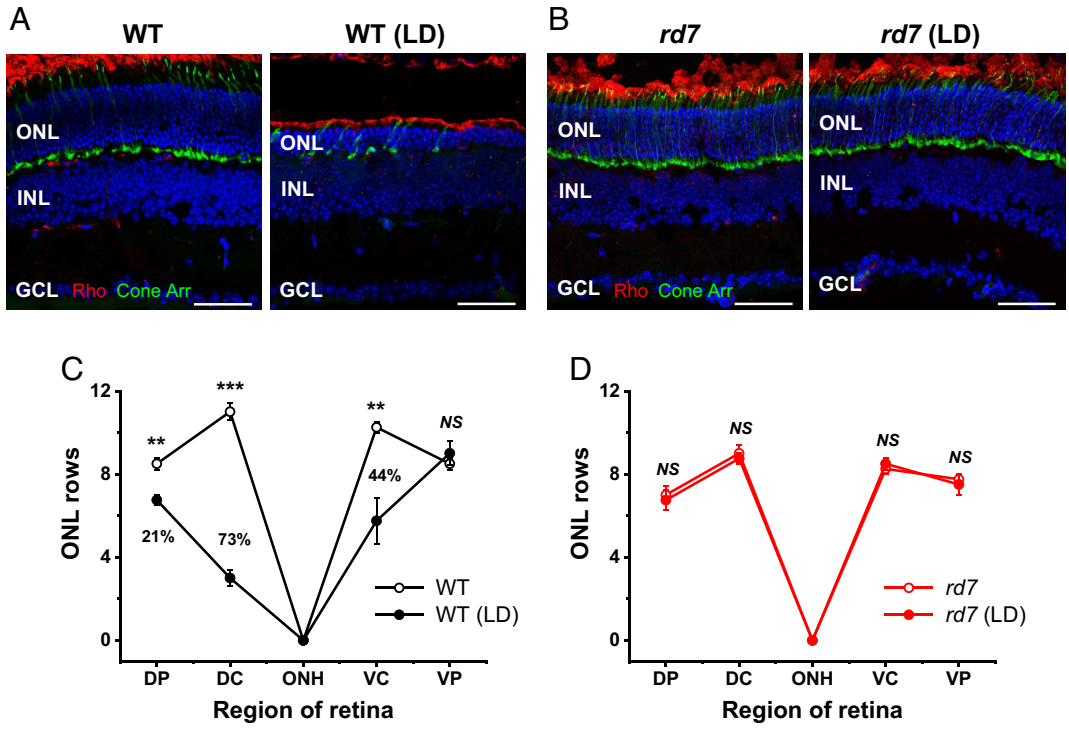

Fig. 1. Rods of *rd7* mice are resistant to LD. (*A* and *B*) Cross-sections of dorsal–central retinas of WT (*A*) and *rd7* (*B*) mice immunostained with anti-rhodopsin (red) and anti-cone arrestin (green) antibodies. Photoreceptor nuclei were counterstained with DAPI (blue). Four-month-old WT control (*A*) and *rd7* (*B*) animals were either unexposed (*Left*) or exposed to bright white light (15 kLux) for 8 h (*Right*). ONL: outer nuclear layer, INL: inner nuclear layer, GCL: ganglion cell layer. (Scale bar, 50 μm.) (*C* and *D*) ONL thickness [quantified as the number of rows of photoreceptor nuclei (ONL rows)] in four regions of the retina from WT (*C*) and *rd7* (*D*) animals either unexposed (open circles) or exposed to 15 kLux white light for 8 h (closed circles). DP: dorsal–peripheral, DC: dorsal–central, ONH: optic nerve head, VC: ventral–central, VP: ventral–peripheral. Values are means ± SEM (n = 4 in all cases). Statistical significances of the data are presented as $^{**}P < 0.01$, $^{***}P < 0.001$, or *NS* (not significant, $P > 0.05$). Numbers show percentages of ONL thickness reduction in light-exposed mice compared to controls.

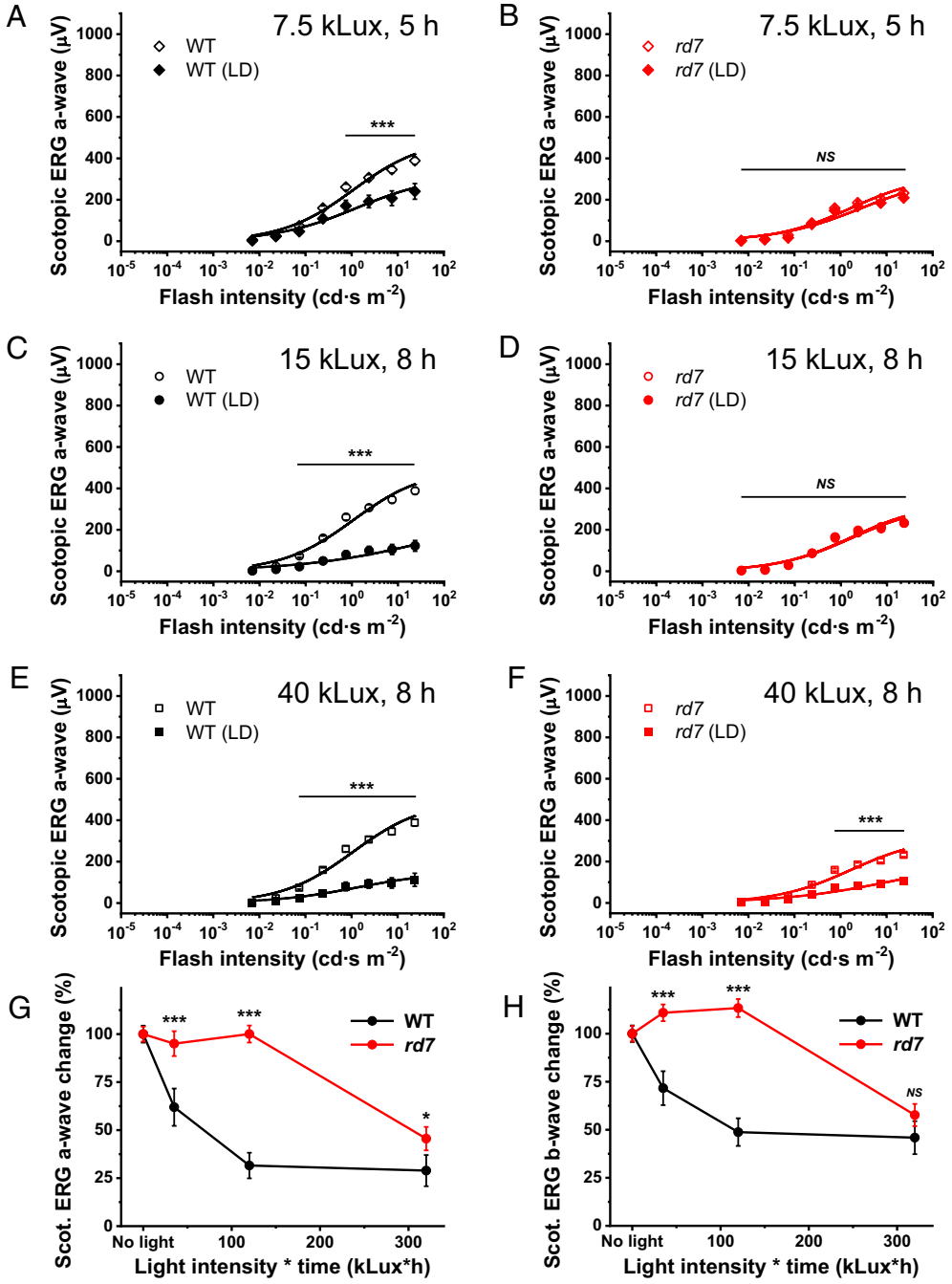

Fig. 2. Physiological characterization of rod susceptibility to LD in WT and *rd7* mice by in vivo ERG. (*A* and *B*) Averaged scotopic intensity–response functions (mean ± SEM) for WT (*A*) and *rd7* (*B*) mice either unexposed (open diamonds) or exposed to 7.5 kLux white light for 5 h (closed diamonds). n = 10 to 12 (control) or 8 to 14 (*rd7*) per group. (*C* and *D*) Averaged scotopic intensity–response functions (mean ± SEM) for WT (*C*) and *rd7* (*D*) mice either unexposed (open circles) or exposed to 15 kLux white light for 8 h (closed circles). n = 10 to 12 (control) or 10 to 14 (*rd7*) per group. (*E* and *F*) Averaged scotopic intensity–response functions (mean ± SEM) for WT (*E*) and *rd7* (*F*) mice either unexposed (open squares) or exposed to 40 kLux white light for 8 h (closed squares). n = 10 to 12 (control) or 10 to 14 (*rd7*) per group. Data in (*A*–*F*) were fitted with hyperbolic Naka-Rushton functions. Error bars for some points in (*A*–*F*) are smaller than the symbol size. (*G* and *H*) Quantification of maximal scotopic ERG a-wave (*G*) or b-wave (*H*) (both recorded with green test flash of 23.5 cd s m^{-2}) changes in WT and *rd7* mice at different LD conditions. The data were normalized to responses obtained from unexposed mice (i.e., no LD). Values are means ± SEM. Statistical significances of the data in (*A*–*H*) are shown as **P* < 0.05, ****P* < 0.001, or *NS* (not significant, *P* > 0.05).

b-waves (*SI Appendix*, Fig. S1), comparable to that observed in the intermediate LD experiment. At this very bright light intensity, we observed reduction of both ERG components in *rd7* mice (a-waves in Fig. 2*F*). Quantitative analysis of the ERG results obtained from the three different light regimens shows that the rods of *rd7* mice are substantially more resistant to photodamage than their WT counterparts (Fig. 2 *G* and *H*). We conclude that *Nr2e3* knockout protects rod integrity and function over a wide range of light exposures, resulting in the structural and functional preservation of cone cells as well.

***Nr2e3* Knockout Protects Photoreceptors from Degeneration in *Rho*$^{-/-}$ Mice.** To determine whether *Nr2e3* deficiency can prevent photoreceptor degeneration in a mouse model of RP, we crossed *rd7* mice with *Rho*$^{-/-}$ mice, which lack rhodopsin and consequently fail to form rod outer segments (29). *Rho*$^{-/-}$ mice experience a progressive loss of rods. While cones are not directly affected by the deletion of rhodopsin and initially develop normally, rod death eventually leads to secondary cone loss (26).

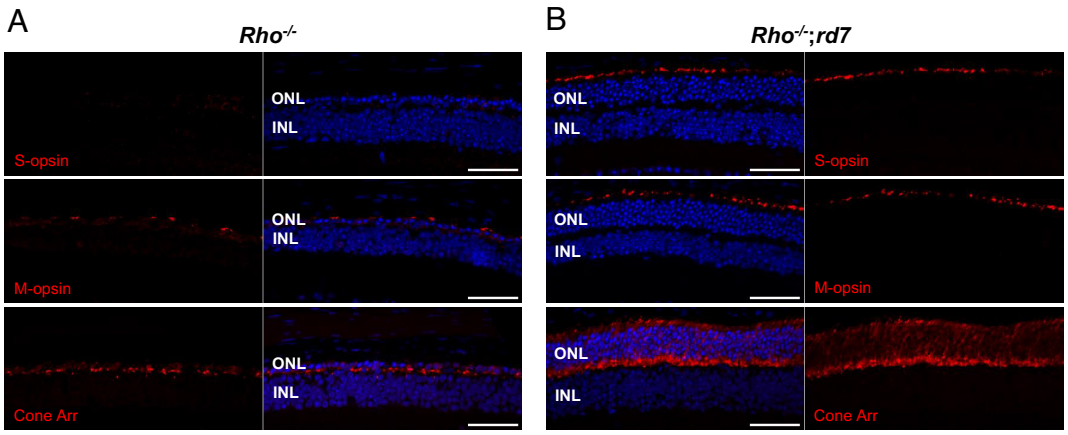

Fig. 3. Preservation of cone photoreceptors in 4-mo-old *Rho*$^{-/-}$;*rd7* mice. (*A* and *B*) Cross-sections of ventral–central (*Top*) and dorsal–central (*Middle* and *Bottom*) retinas of *Rho*$^{-/-}$ (*A*) and *Rho*$^{-/-}$;*rd7* (*B*) mice immunostained with anti-S-opsin (*Top*), anti-M-opsin (*Middle*), or anti-cone arrestin (*Bottom*) antibodies (red). Photoreceptor nuclei in (*A* and *B*) were counterstained with DAPI (blue). ONL: outer nuclear layer, INL: inner nuclear layer. (Scale bar, 50 μm.)

Consistent with previous results (26), we observed only a single remaining row of photoreceptor nuclei in the outer nuclear layer (ONL) of 4-mo-old *Rho*$^{-/-}$ mice (Fig. 3*A*). In contrast, the ONL of *Rho*$^{-/-}$;*rd7* mice was largely preserved (Fig. 3*B*) even though rods still lacked outer segments (*SI Appendix*, Fig. S2). Moreover, while both S- and M-cone opsins were barely detectable in cone outer segments of *Rho*$^{-/-}$ mice (Fig. 3 *A*, *Top* and *Middle* rows), both visual pigments were still abundantly expressed in cones of *Rho*$^{-/-}$;*rd7* mice (Fig. 3 *B*, *Top* and *Middle* rows). Immunostaining for cone arrestin further confirmed the presence of severe cone degeneration in *Rho*$^{-/-}$ mice, while showing relatively preserved cone morphology in *Rho*$^{-/-}$;*rd7* mice (Fig. 3 *A* and *B*, *Bottom* rows). To quantify the extent of photoreceptor rescue by *rd7*, we counted nuclei in the ONL of 4-mo-old *Rho*$^{-/-}$ and *Rho*$^{-/-}$;*rd7* mice. We found that the ONL of *Rho*$^{-/-}$;*rd7* mice contained >five-fold more photoreceptor nuclei (105 ± 14 nuclei/100-μm segment of retina; n = 3) than that of *Rho*$^{-/-}$ mice (20 ± 0.5 nuclei/100 μm; n = 3), indicating a powerful neuroprotective effect of the *rd7* mutation (***P < 0.001; n = 3; independent-samples t test). Together, these results indicate that *Nr2e3* knockout potently prolongs the survival of *Rho*$^{-/-}$ rods and prevents secondary cone death.

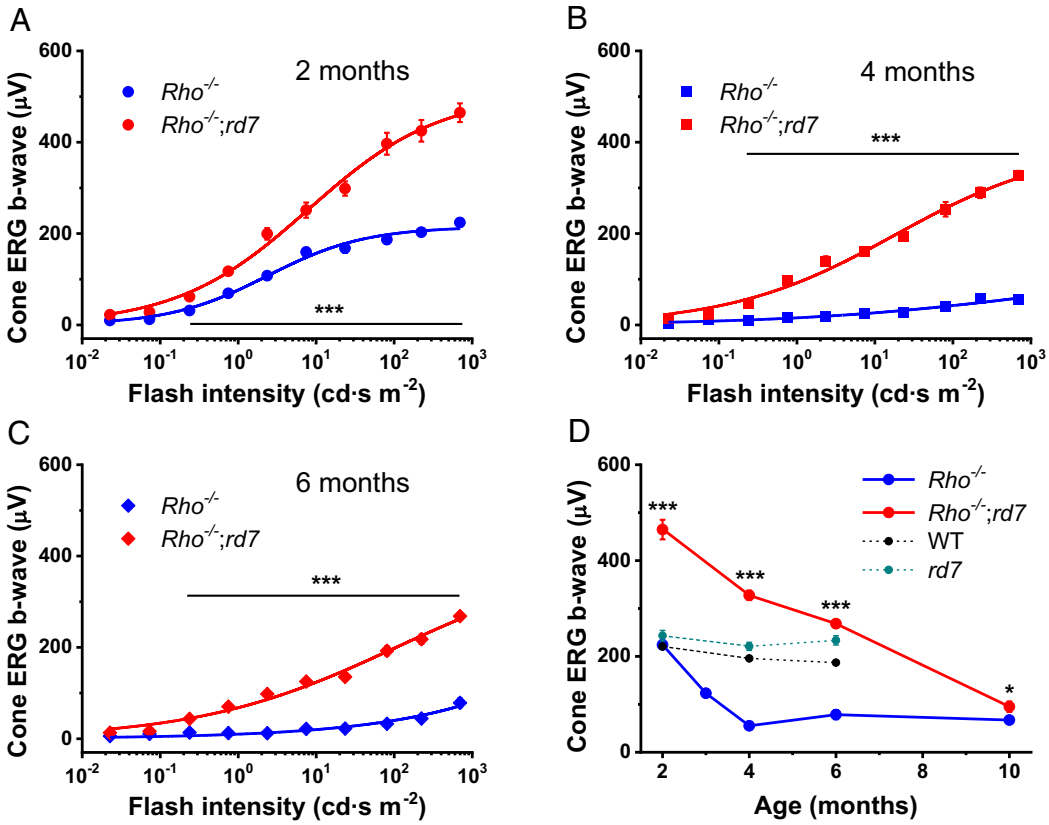

Fig. 4. Preservation of cone function in *Rho*$^{-/-}$;*rd7* mice. (*A*–*C*) Averaged cone ERG b-wave intensity–response functions (mean ± SEM) for *Rho*$^{-/-}$ and *Rho*$^{-/-}$;*rd7* mice at 2 mo (*A*), 4 mo (*B*), and 6 mo (*C*) of age. Data in (*A*–*C*) were fitted with hyperbolic Naka-Rushton functions. n = 6 to 8 (*Rho*$^{-/-}$) or 6 to 10 (*Rho*$^{-/-}$;*rd7*) per group. (*D*) Quantification of cone maximal ERG b-wave (recorded with white test flash of 700 cd s m^{-2}) at multiple postnatal time points. n = 6 (WT control), n = 6 to 8 (*rd7* control), n = 6 to 8 (*Rho*$^{-/-}$), n = 6 to 10 (*Rho*$^{-/-}$;*rd7*) per group. Values are means ± SEM. Error bars for some points in (*A*–*D*) are smaller than the symbol size. In (*A*–*D*), statistical significances of the data (between *Rho*$^{-/-}$ and *Rho*$^{-/-}$;*rd7* lines) are shown as *P < 0.05, or ***P < 0.001.

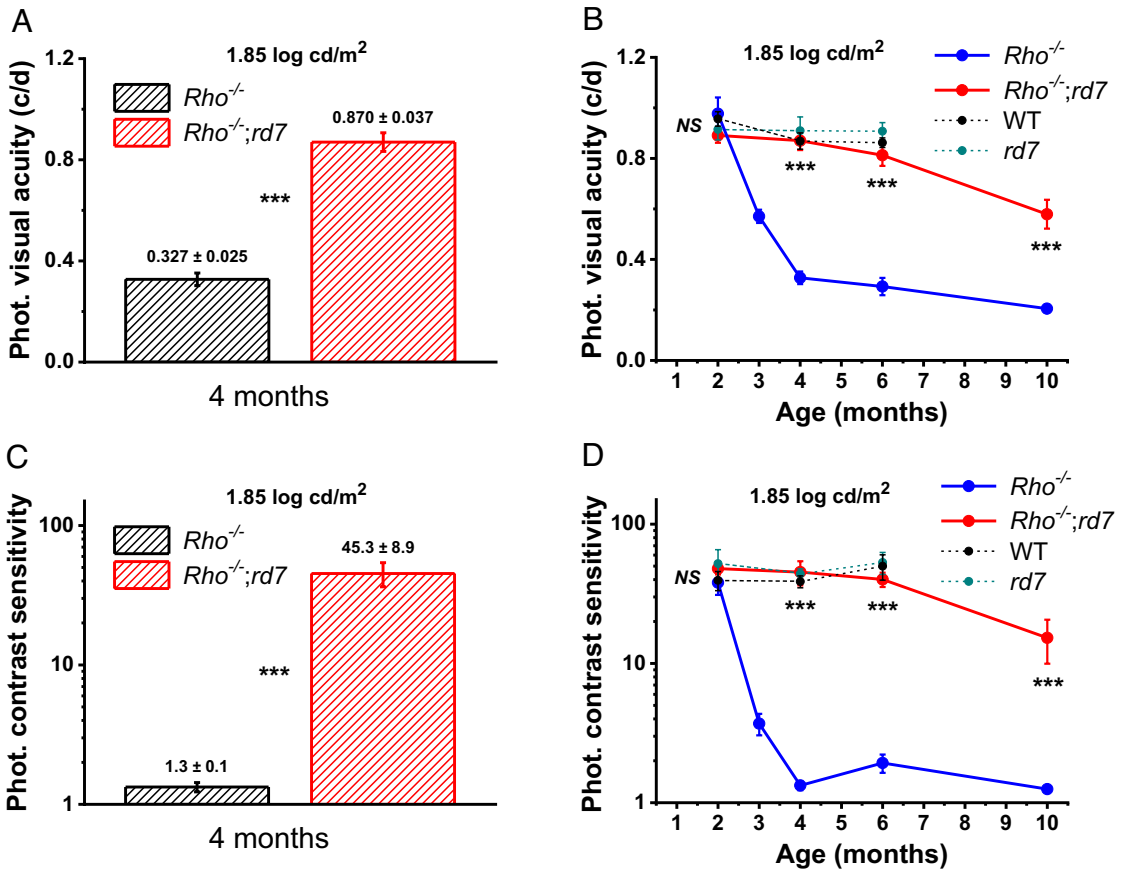

Fig. 5. Long-term preservation of photopic vision in *Rho*$^{-/-}$;*rd7* mice. Quantification of changes in photopic visual acuity (*A* and *B*) and photopic contrast sensitivity (*C* and *D*) at multiple postnatal time points. Raw data, as shown in panels (*A*) and (*C*) for 4-mo-old mice, were derived from optomotor responses to rotating gratings under photopic (1.85 log cd m^{-2}) background illumination conditions. n = 3 (WT control), n = 4 (*rd7* control), n = 4 (*Rho*$^{-/-}$), n = 3 to 5 (*Rho*$^{-/-}$;*rd7*) mice per group. Values are means ± SEM. Error bars for some points in (*B*) and (*D*) are smaller than the symbol size. In (*B*) and (*D*), statistical significances of the data (between *Rho*$^{-/-}$ and *Rho*$^{-/-}$;*rd7* lines) were $P > 0.05$ (*NS*) at 2 mo and ***$P < 0.001$ for all other ages.

Cone Function and Photopic Vision Are Preserved in *Nr2e3*-Deficient *Rho*$^{-/-}$ Mice. We next used ERG to monitor the progression of photopic functional decline in *Rho*$^{-/-}$ and *Rho*$^{-/-}$;*rd7* mice. Despite the preservation of rod cell bodies in *Rho*$^{-/-}$;*rd7* animals (Fig. 3), the lack of rod visual pigment prevented these cells from responding to light and, as a result, rod-driven ERG responses were absent in this model. Consistent with the morphological changes described above, the M-cone-driven ERG b-wave was normal in 2-mo-old *Rho*$^{-/-}$ mice but declined rapidly and was barely detectable by 4 mo of age (Fig. 4 *A*–*D*). The cone b-wave responses in *Rho*$^{-/-}$;*rd7* animals were substantially larger than those in controls at 2 mo, possibly reflecting synaptic remodeling and plasticity in the retinas of *Rho*$^{-/-}$;*rd7* mice in the absence of functional rods, or altered outer retina resistance due to the lack of rod outer segments. Strikingly, M-cone function was largely preserved up to 6 mo of age in *Rho*$^{-/-}$;*rd7* mice (Fig. 4 *A*–*D*). At 6 mo of age, *Rho*$^{-/-}$;*rd7* cone responses were comparable to those in control WT and *rd7* mice (Fig. 4*D*) and significantly higher than those in *Rho*$^{-/-}$ mice. Eventually, cone function in *Rho*$^{-/-}$;*rd7* mice declined, yet photopic responses remained significantly higher ($^*P < 0.05$) than those in the *Rho*$^{-/-}$ group out to 10 mo of age.

We also evaluated visual acuity and contrast sensitivity in the same cohorts of mice by measuring their optomotor head-turning responses to rotating vertical grating stimuli (30, 31). We found that visual acuity was ~3 times greater in 4-mo-old *Rho*$^{-/-}$;*rd7* mice than in *Rho*$^{-/-}$ animals under bright light (photopic) conditions in which vision is exclusively mediated by cones (Fig. 5*A*). Photopic visual acuity was well-preserved in *Rho*$^{-/-}$;*rd7* mice for up to 10 mo (Fig. 5*B*), while it deteriorated rapidly in *Rho*$^{-/-}$ animals. Notably, photopic visual acuity was preserved to a greater extent than cone ERG responses (Fig. 4*D*), which might be explained by the compensatory plasticity of overall mouse visual function, as observed previously (32).

The photopic contrast sensitivity of *Rho*$^{-/-}$;*rd7* mice was preserved to an even greater extent than visual acuity and was ~35-fold higher than that in *Rho*$^{-/-}$ animals at 4 mo of age (Fig. 5*C*). This difference persisted for up to 10 mo (Fig. 5*D*). Together, these results demonstrate that *Nr2e3* knockout potently preserves photopic visual function in *Rho*$^{-/-}$ mice.

***Nr2e3* Deficiency Promotes Long-Term Rod and Cone Survival and Function in *rd10* Mice.** We next evaluated the neuroprotective effects of *Nr2e3* deficiency in another mouse RP model, *rd10*. These mutant mice have greatly reduced levels of the catalytic subunit of phosphodiesterase 6B and hence impaired rod phototransduction (24, 33). They also experience more rapid rod degeneration than *Rho*$^{-/-}$ mice, with secondary cone loss reaching completion by about 2.5 mo of age (34, 35). We crossed *rd10* and *rd7* mice to generate double mutants and analyze the structure and function of their rods and cones.

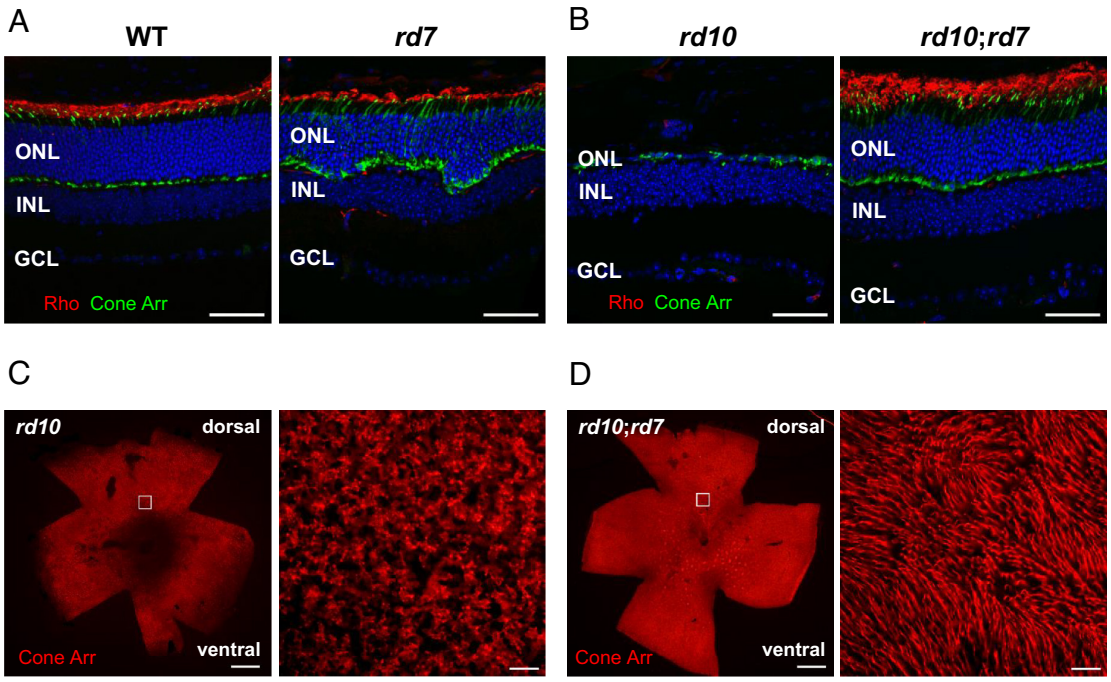

Fig. 6. Cone survival in 4-mo-old *rd10*;*rd7* mice. (*A* and *B*) Cross-sections of dorsal–central retinas of WT and *rd7* controls (*A*) and *rd10* and *rd10*;*rd7* (*B*) mice immunostained with anti-rhodopsin (red) and anti-cone arrestin (green) antibodies. Photoreceptor nuclei were counterstained with DAPI (blue). ONL: outer nuclear layer, INL: inner nuclear layer, GCL: ganglion cell layer. (Scale bar, 50 μm.) (*C* and *D*) Representative retinal flatmounts from *rd10* (*C*) and *rd10*;*rd7* (*D*) animals immunostained with anti-cone arrestin (red) antibody (*Left* panels; Scale bar, 1,000 μm). *Right* panels in (*C*) and (*D*) show higher magnification images obtained from dorsal–central regions outlined with white squares. (Scale bar, 50 μm.)

Similar to the case with $Rho^{-/-}$ mice, we found that *Nr2e3* knockout greatly suppressed the degeneration of photoreceptors in 4-mo-old *rd10* mice, as evidenced by immunohistochemical staining of retinal cross-sections (Fig. 6 *A* and *B*). Unlike in *rd10* mice, the outer segments of *rd10;rd7* rods could be readily observed by anti-rhodopsin immunostaining and appeared healthy. The cones of *rd10*;*rd7* mice were likewise preserved, as demonstrated by cone arrestin staining of retinal flat-mounts (Fig. 6 *C* and *D*). To quantify the extent of cellular rescue by *rd7*, we counted the nuclei in the ONL of 4-mo-old *rd10* and *rd10*;*rd7* mice. We found that there were ~13-fold more nuclei in the ONL of *rd10*;*rd7* mice (192 ± 33 nuclei/100 μm; n = 3) compared to that of *rd10* (15 ± 2 nuclei/100 μm; n = 3). The difference was highly significant (**$P < 0.01$, independent-samples t test). The potency of the neuroprotective effect is underscored by the fact that the number of nuclei remaining in the ONL of *rd10*;*rd7* mice was comparable to the number in mice carrying the *rd7* mutation alone (189 ± 22 nuclei/100 μm, n = 3).

In agreement with these histologic findings, rod-driven ERG a-wave responses were dramatically preserved in *rd10*;*rd7* mice at 4 mo of age relative to *rd10* controls (Fig. 7*A*). Scotopic ERG responses of *rd10*;*rd7* mice were indistinguishable from those of *rd7* mice for up to 6 mo. In fact, scotopic function was almost completely preserved up to 10 mo of age (Fig. 7*B*). As expected, maximal ERG a-waves were reduced by ~30% in *rd7* mice as compared to WT animals (Fig. 7*B*), likely due to the slightly lower number of rods in this strain overall (Fig. 2). The same degree of functional preservation was also observed for scotopic ERG b-waves in *rd10*;*rd7* animals (Fig. 7*C*). Remarkably, the accompanying decline of photopic ERG b-wave responses in *rd10* mice was fully corrected by *Nr2e3* knockout as well (Fig. 7*D*). Importantly, physiological rescue also resulted in preservation of scotopic (Fig. 8 *A* and *B*) and photopic (Fig. 8 *C* and *D*) visual acuity and contrast sensitivity in *rd10*;*rd7* mice. Collectively, our findings indicate that *Nr2e3* deficiency preserves long-term rod- and cone-mediated visual function in *rd10* mice.

Discussion

In the present study, we tested the hypothesis that germline mutation of *Nr2e3* (*rd7*) would render rod photoreceptors resistant to degeneration and thereby prevent secondary cone loss. Indeed, mice with mutations in *Nr2e3* show prolonged survival and function of both rods and cones in three mechanistically distinct models of disease: LD, *Rho* mutation, and *Pde6b* (*rd10*) mutation. Together, these findings indicate that the preservation of rods by the deletion of *Nr2e3* might offer a viable approach for preventing secondary cone loss and preserving cone function, a key therapeutic goal in patients with RP.

The protective effect of the *Nr2e3* mutation is unlikely attributable to the absence of NR2E3 protein per se, but rather to the changes in downstream gene expression that result from its loss. In 2005, three groups reported that mutation of *Nr2e3* in mice causes upregulation of a subset of cone genes in rods without significant effects on rod gene expression (19, 20, 36). We subsequently used RNA-seq to compare the transcriptomes of WT and *rd7* mouse retinas and found a total of 480 genes to be significantly dysregulated in adult *rd7* retinas (37). To more closely evaluate these dysregulated genes, we compared this list with the results of another study in which we used RNA-seq to classify mouse genes as rod-enriched, cone-enriched, or not differentially expressed between the two cell types (38). We were able to map 479 of the 480 *rd7*-dysregulated genes onto this second dataset (*SI Appendix*, Table S1). In accordance with the reported role of NR2E3 as a repressor of cone genes in rods, we found that ~37% (154/415) of *rd7*-upregulated genes are cone-enriched. If we restrict our attention to those genes that are markedly upregulated in *rd7* (i.e.,

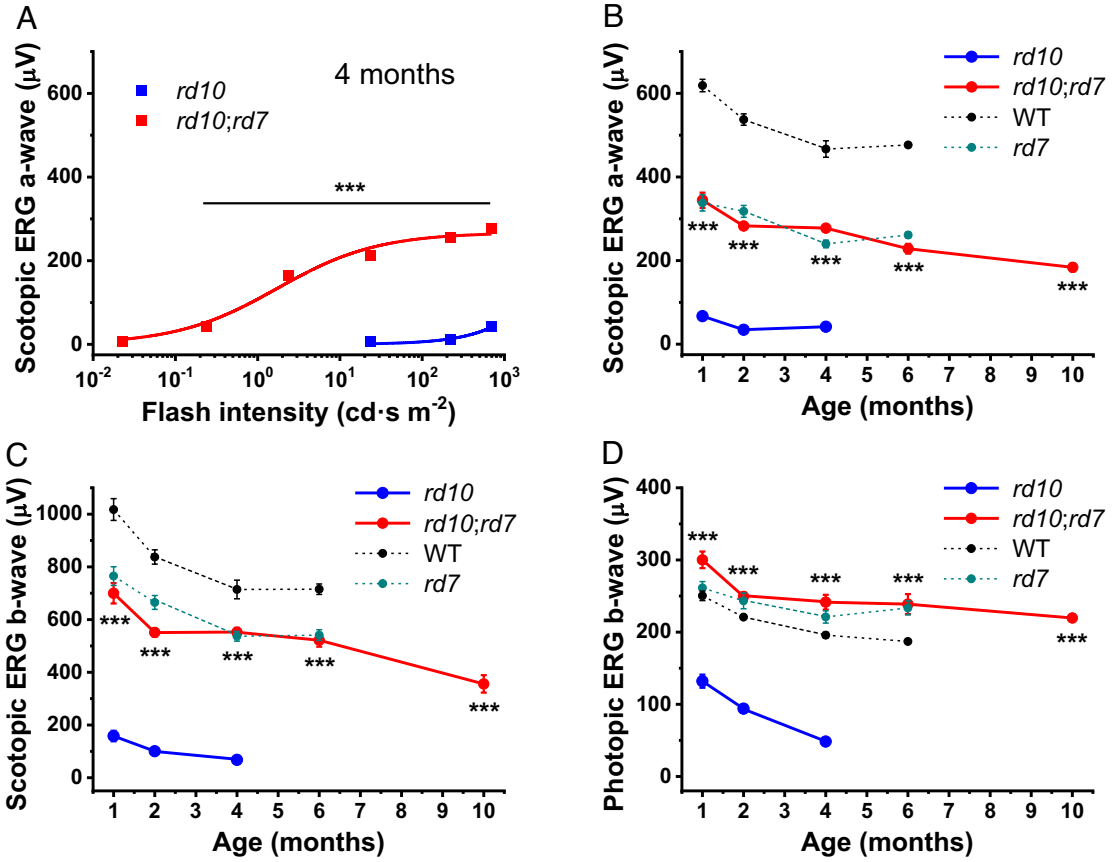

Fig. 7. Preservation of photoreceptor function in *rd10*;*rd7* mice. (*A*) Averaged scotopic ERG a-wave intensity–response functions (mean ± SEM) for *rd10* and *rd10*;*rd7* mice at 4 mo of age. Data were fitted with hyperbolic Naka-Rushton functions. n = 10 (*rd10*) or 12 (*rd10*;*rd7*) per group. (*B–D*) Quantification of scotopic maximal ERG a-wave (*B*) and b-wave (*C*) and photopic maximal ERG b-wave (*D*) (all recorded with white test flash of 700 cd s m^{-2}) at multiple postnatal time points. n = 6 (WT control), n = 6 to 8 (*rd7* control), n = 8 to 10 (*rd10*), n = 4 to 12 (*rd10*;*rd7*) per group. Values are means ± SEM. Error bars for some points in (*B–D*) are smaller than the symbol size. In (*A–D*), statistical significances of the data (between *rd10* and *rd10*;*rd7* lines) were ***$P < 0.001$ for all ages.

≥threefold), we find that ~61% (48/79) are cone-enriched. The majority of the remaining *rd7*-upregulated genes (251/415) are not differentially expressed between WT rods and cones, and the extent of their upregulation is generally minimal (i.e., <threefold). Only a small number (47/479) of *rd7*-dysregulated genes are rod-enriched, and no genes encoding components of the rod phototransduction cascade are affected to a functionally significant extent. Thus, the principal effect of the *rd7* mutation is marked (≥threefold) upregulation of a small set of 79 genes, nearly two-thirds (61%) of which are cone-enriched in the adult mouse.

The upregulation of cone genes in *rd7* rods raises the possibility that the neuroprotective effects we observed might be attributable, at least in part, to replacement of the defective rod gene by upregulation of its cone equivalent. Indeed, one of the most upregulated cone genes in *rd7* rods is *Pde6c* (*SI Appendix*, Table S1), which encodes the catalytic subunit of the cone-specific phosphodiesterase. As shown in two separate studies, transgenic expression of the cone PDE6C protein (also referred to as PDE6α′) in mouse rods can restore phosphodiesterase activity and function in rods lacking PDE6β (39, 40). Thus, morphological and functional rescue of *rd10* rods (which have markedly reduced levels of PDE6β) by *rd7* might be attributable to upregulation of *Pde6c* expression and consequent restoration of phosphodiesterase activity.

At first glance, it might seem that a similar mechanism could account for rescue of the $Rho^{-/-}$ phenotype by the *rd7* mutation. Transcriptome analysis shows a 2.5-fold increase in blue cone opsin (*Opn1sw*) expression in *rd7* retinas (*SI Appendix*, Table S1), suggesting that upregulation of cone opsin expression in $Rho^{-/-}$ rods might restore function and therefore be neuroprotective. However, prior studies showed that there is no upregulation of *Opn1sw* in *rd7* rods, despite the upregulation of various other cone-specific genes in these cells (19). Instead, there is ~twofold increase in the number of blue cones in the *rd7* retina, which likely accounts for the modest increase in *Opn1sw* transcripts detected by whole-retina expression profiling (37). Thus, it appears that *rd7*-mediated rescue of $Rho^{-/-}$ rods occurs despite the absence of opsin expression or detectable outer segments in these cells.

Similarly, it is unlikely that a "gene replacement" mechanism mediates the resistance to LD observed in the *rd7* retina, as light-induced rod cell death is not caused by deficiency of one specific rod gene. Instead, the potent rescue we observe in three different models of photoreceptor degeneration suggests that either a single general neuroprotective mechanism or multiple model-specific mechanisms are operative in *rd7* mice. We propose that these protective effects are likely mediated by the upregulation of one or more cone genes in *rd7* rods. Future studies will be directed toward identifying the gene(s) mediating these therapeutic effects.

While promising, these results are only a step toward the development of a successful gene-independent therapy for RP. For obvious reasons, it is not possible to treat human RP patients by inducing germline mutations in *NR2E3*. It will therefore be necessary to devise a strategy to acutely knock out *NR2E3* in mature rods. One strategy would be to use CRISPR-Cas9 technology to achieve knock out. Such a strategy was used previously to knock out mouse *Nrl,* thereby delaying degeneration in multiple mouse

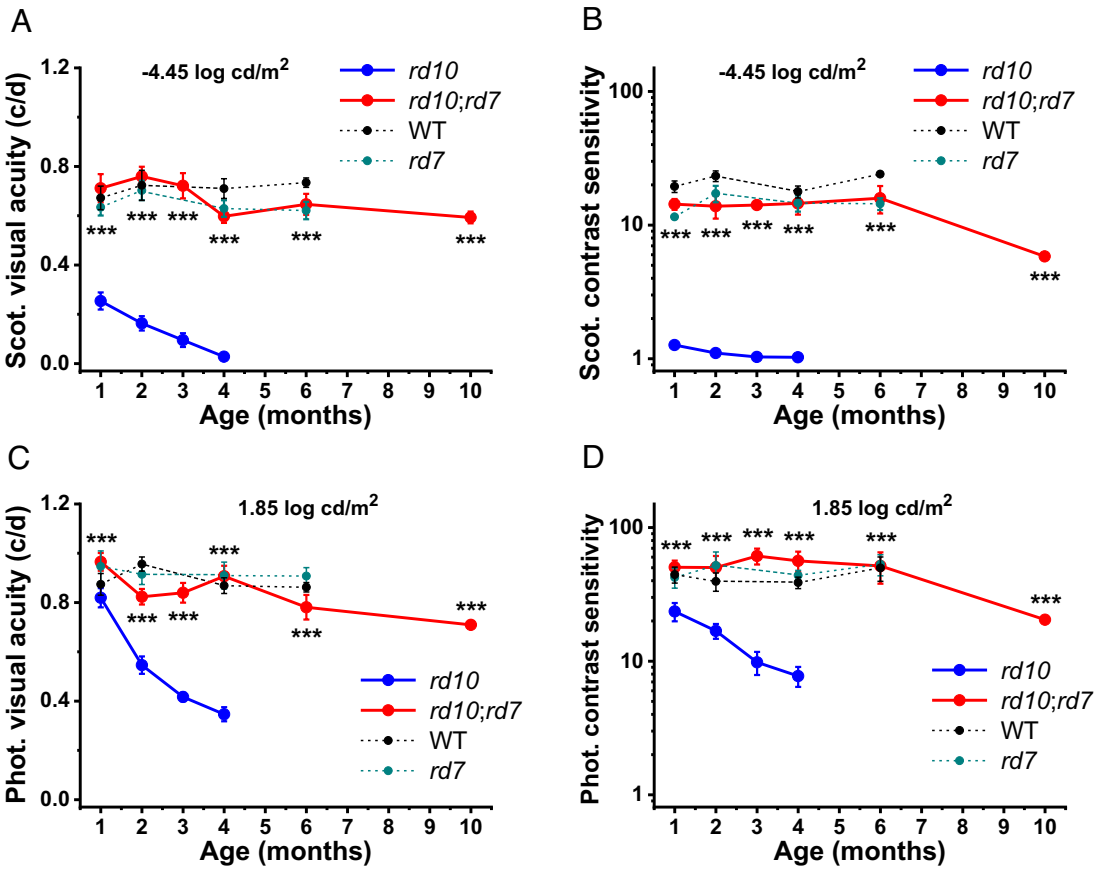

Fig. 8. Long-term preservation of scotopic and photopic vision in *rd10;rd7* mice. Quantification of scotopic visual acuity (*A*), scotopic contrast sensitivity (*B*), photopic visual acuity (*C*), and photopic contrast sensitivity (*D*) at multiple postnatal time points. Data were derived from mouse optomotor responses to rotating gratings under scotopic (−4.45 log cd m^{-2}) or photopic (1.85 log cd m^{-2}) background illumination conditions. n = 3 (WT control), n = 4 (*rd7* control), n = 4 (*rd10*), n = 3 to 5 (*rd10;rd7*) mice per group. Values are means ± SEM. Error bars for some points in (*A–D*) are smaller than the symbol size. In (*A–D*), statistical significances of the data (between *rd10* and *rd10;rd7* lines) were ***$P < 0.001$ for all ages.

models of RP (9, 11). Alternatively, it might be possible to target *NR2E3* using antisense oligonucleotides, an approach which has proven successful in the treatment of neurologic disease (41–43). The transcriptomic and therapeutic effects of acute *NR2E3* knockout or knockdown would first need to be evaluated in mice and human retinal organoids.

Another outstanding issue is that loss of *Nr2e3* produces distinct phenotypes in mice and humans (19). While *rd7* mice show relatively modest changes in rod gene expression and exhibit no evidence of enhanced sensitivity to short-wavelength light, humans with mutations in *NR2E3* have enhanced S-cone syndrome characterized by a supranormal ERG response to short-wavelength light (44). These observations suggest that the function of NR2E3 is not entirely conserved between the mouse and human and that *NR2E3*-mutant human rods may be transfated into supernumerary blue cones. Indeed, a recent analysis of *NR2E3*-mutant human retinal organoids shows an absence of rhodopsin-expressing rods and a late transfating of "divergent rods" into blue cones (45). Clearly, the therapeutic potential of targeting *NR2E3* will require further study in human cells.

A third challenge is that humans with *NR2E3* mutations exhibit a late-onset, slowly progressive photoreceptor degeneration. It is therefore possible that therapeutic targeting of *NR2E3* in patients will cause a similar degeneration. However, this concern may be unwarranted, because acute knockout of *Nr2e3* in mature rods is expected to cause a much milder perturbation of gene expression than germline knockout. Prior studies showed that germline knockout of mouse *Nrl* alters the expression of thousands of genes and results in a complete transfating of rods into blue cones (46, 47), whereas acute knockout of *Nrl* in mature rods changes the expression of only 146 genes (11). Thus, acute *Nr2e3* knockout in mature rods is likely to yield a much milder phenotype than germline knockout while still retaining therapeutic efficacy.

Two other groups have recently begun to evaluate *Nr2e3* as a potential therapeutic target for treatment of RP. Nakamura et al. reported that a small molecule inhibitor of NR2E3 (photoregulin3) prevents photoreceptor degeneration in a mouse model (48, 49). On the other hand, Li et al. suggested that overexpression of *Nr2e3* slows disease progression in multiple mouse RP models (50). The results presented here confirm *Nr2e3* as a promising therapeutic target, but they contradict some aspects of the prior work. Nakamura et al. found that photoregulin3 causes widespread downregulation of rod genes (48). In contrast, our findings indicate that germline *Nr2e3* knockout leads to upregulation of cone genes without major effects on rod gene expression. This finding suggests that photoregulin3 may not act by simply inhibiting NR2E3 function but via a more complicated mechanism. Similarly, Li et al. suggested that adeno-associated virus-mediated overexpression of *Nr2e3* preserves ONL thickness in four mouse models of RP (50). However, the histologic images in their paper (Fig. 4*A* in ref. 50) show no difference in ONL thickness between treated mice and controls. Moreover, our results indicate that *Nr2e3* knockout prevents photoreceptor degeneration, a finding that is difficult to reconcile with Li et al.'s reported overexpression results.

Resolving these discrepancies is of great significance because efforts are underway to translate this finding into a human therapy (51).

Materials and Methods

Animals. All experiments were performed in accordance with the NIH Guide for the Care and Use of Laboratory Animals and the Association for Research in Vision and Ophthalmology Statement for the Use of Animals in Ophthalmic and Vision Research and were approved by the Institutional Animal Care and Use Committee of UC Irvine and Washington University in St. Louis. All mice used in this study, with the exception of those used in LD experiments, were homozygous for the Met-450 allele of the *Rpe65* gene as determined by a genotyping protocol published elsewhere (52). All mice were confirmed to be free of the *Crb1*^{rd8} mutation (53). The retinal degeneration 7 (*rd7*) strain (homozygous for the Met-450 allele of *Rpe65*) was obtained from The Jackson Laboratory (*rd7*;*Rpe65*$^{Met\text{-}450/Met\text{-}450}$; strain # 004643). For LD experiments, *rd7* animals were crossed with 129S2/Sv mice (which carry the Leu-450 variant of *Rpe65*; Charles River Laboratories) to generate *rd7*;*Rpe65*$^{Leu\text{-}450/Leu\text{-}450}$ mice. These mice were subsequently maintained on a mixed C57Bl6/J x 129S2/Sv genetic background. Mice with a knockout of the rhodopsin gene (*Rho*$^{-/-}$) were described previously (26). Animals with the missense R560C mutation in phosphodiesterase 6 β-subunit (*Pde6b*$^{R560C/R560C}$) causing the retinal degeneration 10 (*rd10*) phenotype were described previously (33). Both *Rho*$^{-/-}$ and *rd10* lines were crossed with *rd7*;*Rpe65*$^{Met\text{-}450/Met\text{-}450}$ mice to generate *Rho*$^{-/-}$;*rd7* and *rd10*;*rd7* double mutants and corresponding *Rho*$^{-/-}$ and *rd10* controls on the same genetic backgrounds. All control and experimental mice of either sex were used at 1 to 10 mo of age. Animals were fed with standard chow (LabDiet 5053; Purina Mills) and raised under standard 12-h dark/light cyclic conditions.

Immunohistochemistry. Preparation of histologic sections was performed as previously described (54). To facilitate identification of the dorsal portion of the retina, the dorsal cornea was marked by cautery (Bovie) immediately prior to enucleation. The eye was then punctured with a 33G needle and fixed in 4% PFA for 5 min. The cornea and lens were then removed, and the eye cup was fixed for an additional 40 min at room temperature. Eyecups were cryoprotected overnight in a solution of 30% sucrose in phosphate-buffered saline and then embedded in Optimal Cutting Temperature compound (Tissue-Tek). Retinal sections were cut at 14-μm thickness using a Leica CM1520 cryostat, mounted on Fisher Superfrost Plus slides, and stored at −20 °C until further use. Immunohistochemical staining was performed with the following primary antibodies: anti-M-opsin (1:200 dilution; Millipore, AB5405), anti-S-opsin (1:600; Millipore, AB5407), anti-rhodopsin (1:200; 4D2 was a kind gift from Robert Molday, University of British Columbia, Vancouver, Canada), and anti-cone arrestin (1:2,000; Millipore, AB15282). For anti-rhodopsin staining, an additional blocking step was performed using AffiniPure donkey anti-mouse Fab fragments (1:10, Jackson Immuno Research) prior to the primary antibody incubation. Secondary antibodies (1:1,000, Invitrogen) included Alexa Fluor 555 donkey anti-mouse and Alexa Fluor 488 or 555 donkey anti-rabbit. Sections were stained for 30 s with DAPI (10 μg/mL, Sigma) and mounted with Vectashield antifade mounting media (vectorlabs). Confocal images at 400× were taken as z-stacks on a Zeiss 880 laser-scanning confocal microscope in the Washington University Center for Cellular Imaging (WUCCI).

Whole-mount retinas were prepared as described (55). Briefly, eyes were marked and removed as with tissue sections. After excising the cornea, a small cut was made to mark the dorsal retina, and the sclera was then removed. Retinas were fixed in 4% PFA for 30 min at room temperature before proceeding with immunohistochemical staining using the primary antibodies listed in above. Before mounting, the lens was removed, and four small incisions were made to permit flattening of the retina. Retinal whole mounts were imaged at 25× magnification on an Olympus BX51 microscope.

Quantification of Photoreceptors. Photoreceptor nuclei were quantified in a central region of the retina adjacent to the optic nerve head. Images of representative vertical retina cross-sections were obtained from three mice for each genotype at 400× magnification. Nuclei in the ONL were counted across the entire image field (295 μm) using the Cell Counter plugin in ImageJ. The counts were then normalized (nuclei per 100-μm length of ONL) and statistically compared by independent two-tailed Student's *t* tests.

LD Experiments. Pupils of WT (*Rpe65*$^{Leu\text{-}450/Leu\text{-}450}$) and *rd7*;*Rpe65*$^{Leu\text{-}450/Leu\text{-}450}$ mice were dilated with a drop of 1% atropine sulfate, and the animals were placed into cages with a white, light-reflective coating. Each cage was divided into four equal compartments with transparent plexiglass dividers. To prevent grouping, every animal was kept in its own compartment for the duration of the experiment. Mice were exposed to broad-spectrum white light emitted by clusters of LEDs placed on top of each cage, under three different intensity regimens: 7.5 kLux for 5 h, 15 kLux for 8 h, or 40 kLux for 8 h. The animals had full access to food and water during light exposure. During light exposure, atropine sulfate was applied to mouse eyes every 2 h to keep the pupils dilated. After light exposure, animals were returned to their normal cages and kept under standard 12-h light/dark cyclic conditions for 1 wk, prior to ERG recordings and collection of tissue for histologic analysis.

In Vivo Electroretinography (ERG). Mice were dark-adapted overnight and anesthetized with an intraperitoneal injection of ketamine (100 mg/kg) and xylazine (4 mg/kg). Pupils were dilated with a drop of 1% atropine sulfate. Mouse body temperature was maintained at 37 °C with a heating pad. ERG a-wave and b-wave responses were measured from both eyes by contact corneal electrodes held in place by a drop of Gonak solution (Akorn). Full-field ERGs were recorded with a UTAS BigShot apparatus (LKC Technologies) using Ganzfeld-derived test flashes of calibrated green 530 nm LED light (within a range from 2.2×10^{-5} cd s m^{-2} to 23.5 cd s m^{-2}) or white light generated by the Xenon Flash tube (from 80.7 cd s m^{-2} to 700 cd s m^{-2}), as previously described (56).

Optomotor Responses. Mouse visual acuity and contrast sensitivity were measured with the OptoMotry system (Cerebral Mechanics) using a two-alternative forced-choice protocol (31), as previously described (57). Optomotor responses were measured under two background illumination conditions: scotopic (−4.45 log cd m^{-2}) or photopic (1.85 log cd m^{-2}). For scotopic conditions, background monitor luminance was controlled by neutral density filters.

Visual acuity was defined as the threshold for spatial frequency (F_s) of sine-wave gratings stimuli with 100% contrast and measured at a speed (S_p) of 6.3 deg/s for scotopic or 12.0 deg/s for photopic illumination conditions. In this mode, F_s was gradually increased by an automated protocol until its threshold was determined. Temporal frequency (F_t) was automatically adjusted by the computer program, based on the following equation: $F_t = S_p \cdot F_s$ (31). Contrast sensitivity was defined as the inverse of contrast threshold for optomotor responses. In this mode, contrast of the stimuli was gradually decreased by the computer until its threshold was reached. For scotopic illumination conditions, F_s was fixed at 0.128 cyc/deg, F_t was set to 0.8 Hz, and S_p was kept at 6.3 deg/s. For photopic conditions, F_s was fixed at 0.128 cyc/deg, F_t was set to 1.5 Hz, and S_p was kept at 12.0 deg/s.

Statistical Analysis. For all experiments, data were expressed as mean ± SEM and analyzed with the independent two-tailed Student's *t* test (using an accepted significance level of $P < 0.05$).

Data, Materials, and Software Availability. All study data are included in the article and/or *SI Appendix*.

ACKNOWLEDGMENTS. This work was supported by a grant from the Washington University Hope Center for Neurological Disorders and a NIH grants EY033810 (to J.C.C. and V.J.K.) and EY030075 (to J.C.C.). We acknowledge additional support to the Gavin Herbert Eye Institute at the University of California, Irvine, from an unrestricted grant from Research to Prevent Blindness and from an NIH core grant (EY034070). We also acknowledge the use of WUCCI supported by Washington University School of Medicine, The Children's Discovery Institute of Washington University and St. Louis Children's Hospital (CDI-CORE-2015-505 and CDI-CORE-2019-813), and the Foundation for Barnes-Jewish Hospital (3770 and 4642).

1. S. P. Daiger, Identifying retinal disease genes: How far have we come, how far do we have to go? *Novartis Found. Symp.* **255**, 17–27; discussion 27-36, 177-178 (2004).
2. A. I. den Hollander, A. Black, J. Bennett, F. P. Cremers, Lighting a candle in the dark: Advances in genetics and gene therapy of recessive retinal dystrophies. *J. Clin. Invest.* **120**, 3042–3053 (2010).
3. A. Rattner, H. Sun, J. Nathans, Molecular genetics of human retinal disease. *Annu. Rev. Genet.* **33**, 89–131 (1999).
4. M. M. Sohocki *et al.*, Prevalence of mutations causing retinitis pigmentosa and other inherited retinopathies. *Hum. Mutat.* **17**, 42–51 (2001).
5. S. K. Verbakel *et al.*, Non-syndromic retinitis pigmentosa. *Prog. Retin. Eye Res.* **66**, 157–186 (2018).

6. D. T. Hartong, E. L. Berson, T. P. Dryja, Retinitis pigmentosa. *Lancet* **368**, 1795–1809 (2006).
7. D. Benati, C. Patrizi, A. Recchia, Gene editing prospects for treating inherited retinal diseases. *J. Med. Genet.* **57**, 437–444 (2020).
8. D. Wang, P. W. L. Tai, G. Gao, Adeno-associated virus vector as a platform for gene therapy delivery. *Nat. Rev. Drug Discov.* **18**, 358–378 (2019).
9. C. L. Montana *et al.*, Reprogramming of adult rod photoreceptors prevents retinal degeneration. *Proc. Natl. Acad. Sci. U.S.A.* **110**, 1732–1737 (2013).
10. S. M. Moore, D. Skowronska-Krawczyk, D. L. Chao, Targeting of the NRL pathway as a therapeutic strategy to treat retinitis pigmentosa. *J. Clin. Med.* **9**, 2224 (2020).
11. W. Yu *et al.*, Nrl knockdown by AAV-delivered CRISPR/Cas9 prevents retinal degeneration in mice. *Nat. Commun.* **8**, 14716 (2017).
12. T. H. Hsiau *et al.*, The cis-regulatory logic of the mammalian photoreceptor transcriptional network. *PLoS One* **2**, e643 (2007).
13. J. W. Kim *et al.*, NRL-regulated transcriptome dynamics of developing rod photoreceptors. *Cell Rep.* **17**, 2460–2473 (2016).
14. D. A. Bessant *et al.*, A mutation in NRL is associated with autosomal dominant retinitis pigmentosa. *Nat. Genet.* **21**, 355–356 (1999).
15. K. W. Littink *et al.*, Autosomal recessive NRL mutations in patients with enhanced S-cone syndrome. *Genes (Basel)* **9**, 68 (2018).
16. A. J. Mears *et al.*, Nrl is required for rod photoreceptor development. *Nat. Genet.* **29**, 447–452 (2001).
17. K. M. Nishiguchi *et al.*, Recessive NRL mutations in patients with clumped pigmentary retinal degeneration and relative preservation of blue cone function. *Proc. Natl. Acad. Sci. U.S.A.* **101**, 17819–17824 (2004).
18. J. W. Kim *et al.*, NRL-regulated transcriptome dynamics of developing rod photoreceptors. *Cell Rep.* **17**, 2460–2473 (2016).
19. J. C. Corbo, C. L. Cepko, A hybrid photoreceptor expressing both rod and cone genes in a mouse model of enhanced S-cone syndrome. *PLoS Genet.* **1**, e11 (2005).
20. J. Chen, A. Rattner, J. Nathans, The rod photoreceptor-specific nuclear receptor Nr2e3 represses transcription of multiple cone-specific genes. *J. Neurosci.* **25**, 118–129 (2005).
21. N. B. Akhmedov *et al.*, A deletion in a photoreceptor-specific nuclear receptor mRNA causes retinal degeneration in the rd7 mouse. *Proc. Natl. Acad. Sci. U.S.A.* **97**, 5551–5556 (2000).
22. J. S. Wang *et al.*, Chromophore supply rate-limits mammalian photoreceptor dark adaptation. *J. Neurosci.* **34**, 11212–11221 (2014).
23. C. Grimm, A. Wenzel, F. Hafezi, C. E. Remé, Gene expression in the mouse retina: The effect of damaging light. *Mol. Vis.* **6**, 252–260 (2000).
24. B. Chang *et al.*, Two mouse retinal degenerations caused by missense mutations in the beta-subunit of rod cGMP phosphodiesterase gene. *Vis. Res.* **47**, 624–633 (2007).
25. S. Sakami *et al.*, Probing mechanisms of photoreceptor degeneration in a new mouse model of the common form of autosomal dominant retinitis pigmentosa due to P23H opsin mutations. *J. Biol. Chem.* **286**, 10551–10567 (2011).
26. J. Lem *et al.*, Morphological, physiological, and biochemical changes in rhodopsin knockout mice. *Proc. Natl. Acad. Sci. U.S.A.* **96**, 736–741 (1999).
27. Y. Zhang *et al.*, Age-related changes in Cngb1-X1 knockout mice: Prolonged cone survival. *Doc. Ophthalmol.* **124**, 163–175 (2012).
28. A. Wenzel, C. E. Reme, T. P. Williams, F. Hafezi, C. Grimm, The Rpe65 Leu450Met variation increases retinal resistance against light-induced degeneration by slowing rhodopsin regeneration. *J. Neurosci.* **21**, 53–58 (2001).
29. M. M. Humphries *et al.*, Retinopathy induced in mice by targeted disruption of the rhodopsin gene. *Nat. Genet.* **15**, 216–219 (1997).
30. G. T. Prusky, N. M. Alam, S. Beekman, R. M. Douglas, Rapid quantification of adult and developing mouse spatial vision using a virtual optomotor system. *Invest. Ophthalmol. Vis. Sci.* **45**, 4611–4616 (2004).
31. Y. Umino, E. Solessio, R. B. Barlow, Speed, spatial, and temporal tuning of rod and cone vision in mouse. *J. Neurosci.* **28**, 189–198 (2008).
32. H. Leinonen *et al.*, Homeostatic plasticity in the retina is associated with maintenance of night vision during retinal degenerative disease. *Elife* **9**, e59422 (2020).
33. B. Chang *et al.*, Retinal degeneration mutants in the mouse. *Vis. Res.* **42**, 517–525 (2002).
34. M. J. Power *et al.*, Systematic spatiotemporal mapping reveals divergent cell death pathways in three mouse models of hereditary retinal degeneration. *J. Comp. Neurol.* **528**, 1113–1139 (2020).
35. T. Wang *et al.*, The PDE6 mutation in the rd10 retinal degeneration mouse model causes protein mislocalization and instability and promotes cell death through increased ion influx. *J. Biol. Chem.* **293**, 15332–15346 (2018).
36. G. H. Peng, O. Ahmad, F. Ahmad, J. Liu, S. Chen, The photoreceptor-specific nuclear receptor Nr2e3 interacts with Crx and exerts opposing effects on the transcription of rod versus cone genes. *Hum. Mol. Genet.* **14**, 747–764 (2005).
37. Y. Xue *et al.*, The role of retinol dehydrogenase 10 in the cone visual cycle. *Sci. Rep.* **7**, 2390 (2017).
38. A. E. Hughes, J. M. Enright, C. A. Myers, S. Q. Shen, J. C. Corbo, Cell type-specific epigenomic analysis reveals a uniquely closed chromatin architecture in mouse rod photoreceptors. *Sci. Rep.* **7**, 43184 (2017).
39. W. T. Deng *et al.*, Cone phosphodiesterase-6alpha' restores rod function and confers distinct physiological properties in the rod phosphodiesterase-6beta-deficient rd10 mouse. *J. Neurosci.* **33**, 11745–11753 (2013).
40. A. Majumder *et al.*, Exchange of cone for rod phosphodiesterase 6 catalytic subunits in rod photoreceptors mimics in part features of light adaptation. *J. Neurosci.* **35**, 9225–9235 (2015).
41. R. S. Finkel *et al.*, Nusinersen versus sham control in infantile-onset spinal muscular atrophy. *N. Engl. J. Med.* **377**, 1723–1732 (2017).
42. T. M. Miller *et al.*, Trial of antisense oligonucleotide tofersen for SOD1 ALS. *N. Engl. J. Med.* **387**, 1099–1110 (2022).
43. S. A. Ramsbottom *et al.*, Targeted exon skipping of a CEP290 mutation rescues Joubert syndrome phenotypes in vitro and in a murine model. *Proc. Natl. Acad. Sci. U.S.A.* **115**, 12489–12494 (2018).
44. Y. Wang, J. Wong, J. L. Duncan, A. Roorda, W. S. Tuten, Enhanced S-cone syndrome: Elevated cone counts confer supernormal visual acuity in the S-cone pathway. *Invest. Ophthalmol. Vis. Sci.* **64**, 17 (2023).
45. N. K. Mullin *et al.*, Loss of NR2E3 disrupts rod photoreceptor cell maturation causing a fate switch late in human retinal development. bioRxiv [Preprint] (2023). https://doi.org/10.1101/2023.06.30.547279 (Accessed 14 February 2024).
46. J. W. Kim *et al.*, Recruitment of rod photoreceptors from short-wavelength-sensitive cones during the evolution of nocturnal vision in mammals. *Dev. Cell* **37**, 520–532 (2016).
47. L. L. Daniele *et al.*, Cone-like morphological, molecular, and electrophysiological features of the photoreceptors of the Nrl knockout mouse. *Invest. Ophthalmol. Vis. Sci.* **46**, 2156–2167 (2005).
48. P. A. Nakamura *et al.*, Small molecule Photoregulin3 prevents retinal degeneration in the Rho(P23H) mouse model of retinitis pigmentosa. *Elife* **6**, e30577 (2017).
49. P. A. Nakamura, S. Tang, A. A. Shimchuk, S. Ding, T. A. Reh, Potential of small molecule-mediated reprogramming of rod photoreceptors to treat retinitis pigmentosa. *Invest. Ophthalmol. Vis. Sci.* **57**, 6407–6415 (2016).
50. S. Li *et al.*, Nr2e3 is a genetic modifier that rescues retinal degeneration and promotes homeostasis in multiple models of retinitis pigmentosa. *Gene Ther.* **28**, 223–241 (2020), 10.1038/s41434-020-0134-z.
51. NCT05203939, A phase 1/2 study to assess the safety and efficacy of OCU400 for retinitis pigmentosa associated with NR2E3 and RHO mutations and Leber congenital amaurosis with mutation(s) in CEP290 gene (2023). https://clinicaltrials.gov/study/NCT05203939.
52. C. Grimm *et al.*, Constitutive overexpression of human erythropoietin protects the mouse retina against induced but not inherited retinal degeneration. *J. Neurosci.* **24**, 5651–5658 (2004).
53. M. J. Mattapallil *et al.*, The Rd8 mutation of the Crb1 gene is present in vendor lines of C57BL/6N mice and embryonic stem cells, and confounds ocular induced mutant phenotypes. *Invest. Ophthalmol. Vis. Sci.* **53**, 2921–2927 (2012).
54. D. Murphy, S. Kolandaivelu, V. Ramamurthy, P. Stoilov, Analysis of alternative pre-RNA splicing in the mouse retina using a fluorescent reporter. *Methods Mol. Biol.* **1421**, 269–286 (2016).
55. A. Venkatesh, S. Ma, F. Langellotto, G. Gao, C. Punzo, Retinal gene delivery by rAAV and DNA electroporation. *Curr. Protoc. Microbiol.* **Chapter 14**, Unit 14D.4 (2013).
56. A. V. Kolesnikov *et al.*, Retinol dehydrogenase 8 and ATP-binding cassette transporter 4 modulate dark adaptation of M-cones in mammalian retina. *J. Physiol.* **593**, 4923–4941 (2015).
57. C. W. Lai *et al.*, Phosducin-like protein 1 is essential for G-protein assembly and signaling in retinal rod photoreceptors. *J. Neurosci.* **33**, 7941–7951 (2013).